SCIENTIFIC RESEARCH

^{99m}Tc-MAA SPECT/CT IMAGING FOR TREATMENT RESPONSE PREDICTION AFTER ^{90}Y-RADIOEMBOLIZATION IN HCC PATIENTS: COMPARISON WITH POST-TREATMENT 90Y PET/CT

Mai Hong Son[1], Le Quoc Khanh[1], Nguyen Thi Phương[1], Nguyen Thi Nhung[1], Nguyen Thanh Huong[1], Le Duy Hung[1], Le Ngoc Ha[1]

SUMMARY

^{90}Y PET/CT imaging is performed after radioembolization to re-evaluate the resin microsphere distribution and estimate the absorbed radiation dose of target tumor. However, the distribution of 90Y resin microsphere on PET/CT was different from that of 99mTc-MAA simulation and additive role of PET/CT was not well established until now. The purpose of our study is to validate the utility of 90Y PET/CT compared to SPECT/CT simulation in dosimetry and prediction of treatment response.

Material and method: Thirty-four consecutive HCC patients, intermediate and advanced stage who underwent 90Y resin microsphere transarterial embolization (TARE) were recruited in the study. Lung shunt fraction (LSF), tumor to-normal liver uptake ratio (TNr) and absorbed dose for target tumors were estimated on 99m Tc-MAA SPECT/CT and 90Y PET/CT. The patients were followed up after treatment within 3 months (2.8 mo ± 0.84) on contrast- enhanced CT to assess treatment response using mRECIST criteria.

Results: The imaging characteristics of thrombosis uptake was better delineated on PET/CT imaging than SPECT/CT. The agreement and correlation of TNr on PET/CT and SPECT/CT were stronger. Dose delivery to tumor (Dtumor) threshold of 125 Gy estimated on 99mTc-MAA SPECT/CT was more accurate than PET/CT for prediction of treatment response after 90Y-radioembolization in HCC patients with sensitivity of 87.5% and specificity of 90%.

Conclusions: 99mTc-MAA SPECT/CT is superior to PET/CT to predict treatment response after 90Y resin microsphere treatment.

Keywords: *Hepatocellular carcinoma, treatment planning, radioembolization, 90Y resin microspheres, 99mTc-MAA SPECT/CT, 90Y PET/CT.*

Hepatocellular carcinoma (HCC) is one of the most common oncology disease in Asia (1). Transarterial radioembolization (TARE) using 90Y resin or glass microsphere is a treatment modality for HCC in intermediate or advanced stage with portal thrombosis. The goal of radioembolization is to give the higher delivery dose to the tumor while sparing normal liver. Treatment planning imaging with ^{99m}Tc-MAA includes lung shunt fraction and tumor-to-normal liver uptake ratio which are the key for optimizing the delivery dose to the tumor and sparing healthy liver and lung. The partition model with ^{99m}Tc-MAA planar image for estimating the absorbed dose to the targeted tumor before the ^{90}Y-microsphere treatment was well established. Currently, ^{99m}Tc-MAA SPECT/CT was recommended to simulate distribution of ^{90}Y-microsphere. Meanwhile, the dosimetry of ^{99m}Tc-MAA for simulation was different from that of ^{90}Y-microsphere and post-treatment ^{90}Y PET/CT imaging was considered as ''gold standard''. Therefore the simulation results with ^{99m}Tc-MAA SPECT/CT should be validated with ^{90}Y PET/CT post-treatment scan.

Other studies reported that ^{99m}Tc-MAA SPECT/CT had a good correlation with ^{90}Y PET/CT in tumor-to-normal liver uptake ratio and SPET/CT is valuable for detecting extrahepatic uptake for stratifying risk of radiation injury to normal organs (2). To the best of our knowledge, there was limited publication compared ^{99m}Tc-MAA SPECT/CT and ^{90}Y PET/CT in the prediction of treatment response in HCC patients.

Our research aims at evaluating the accuracy of dosimetry using ^{99m}Tc-MAA SPECT/CT and in comparison, with PET/CT in the prediction of treatment response after ^{90}Y-loaded resin microspheres therapy.

MATERIAL AND METHOD

Patients: Thirty-four consecutive HCC patients, intermediate and advanced stage in hospital 108 who underwent ^{90}Y-resin microsphere transarterial embolization (TARE) from May 2017 to December 2019 were recruited in the study. Patients suitable for selection criteria should have a preserved hepatic function (Child-Pugh A) and ECOG status from 0 to 2. The indication for TARE was decided upon by the liver cancer tumor board in 108 Hospital. An informed consent was obtained from each patient before being involved in the study. Patients with main portal branch thrombosis, ECOG status > 2, hepatic cirrhosis with Child-Pugh C or lung shunt fraction higher than 20% were excluded.

Simulation, treatment and response evaluation: Multislice intravenous contrast-enhanced abdominal CT scan was carried out to assess angiographic mapping and the volume of normal liver and targeted tumor. For simulation, diagnostic angiography was done for arterial mapping and selection of optimized catheter position for TARE. 5 mCi of ^{99m}Tc-MAA was injected into the artery supplying hepatic tumor. For tumors located in one segment or supplied by at least two hepatic arteries, the corresponding arteries were chosen for injection of ^{99m}Tc-MAA and planned as targeted arteries.

One hour after injection of ^{99m}Tc-MAA to the target tumors, patients were sent to the nuclear medicine department, 108 Hospital for SPECT/CT image on dual-head gamma camera (Optima 610, GE Healthcare, Milwaukee, WI, USA). The range of ^{99m}Tc-MAA scan should cover both lungs and abdomen. Low energy and high-resolution collimators were used and the energy window was set at 140 ±10 KeV. SPECT image was acquired using 90 projections of step and shoot mode and matrix size 256 x 256. CT image was followed by SPECT with voltage 120kV, tube current 30mA and slice thickness 5mm.

Images were present on axial, sagittal and coronal plane and analyzed on Xeleris 4.0 (GE Healthcare, Milwaukee, WI, USA). On planar imaging, region of interests (ROIs) were drawn on both lungs, whole liver and targeted tumor in liver. On both SPECT/CT and ^{90}Y PET/CT, ROIs were drawn on both lungs, liver and tumor by drawing the margin in every axial slice using Dosimetry toolkit (GE Healthcare, Milwaukee, WI, USA) and PETVCAR respectively. The necrotic part of tumor was excluded in the analysis. Total counts of each ROI on either PET/CT and SPECT/CT image were used to estimate lung shunt fraction % (LSF%) and the ratio of tumor-to-normal liver (TNr) with a formula described on EANM guidelines (3). For tumors supplied by at least two hepatic arteries, TNr mean and TNr of each tumor were estimated. The partition model was applied to estimate the mean absorbed dose for lung (Dlung), normal liver (Dliver) and target tumor (Dtumor). The absorbed dose to tumor should be more than 120Gy, Dlung less than 20Gy and Dliver less than 30Gy (4). For tumors located in a segment or supplied by at least two hepatic arteries, super selective treatment based on the partition model was

done. The Dliver and Dtumor were estimated selectively with corresponding tumor and normal liver.

After estimation of dosimetry for targeted tumor, concordant dose of ^{90}Y resin microspheres (SIR-Sphere, SIRTeX™, Sydney, Australia) was injected to tumor-supplying hepatic arteries. After 6 hours, patients were sent to the nuclear medicine department for post-treatment PET/CT scan. The scan was performed with the protocol described in the previous study (5). The imaging characteristics including pattern of tumor uptake, necrosis, thrombosis uptake in SPECT/CT and post-treatment ^{90}Y PET/CT were interpreted by two experienced nuclear physicians in the hospital and consensus was made. ROIs were put on both lungs, liver including tumor and targeted tumors to estimate the LFS % and TNr. We compared TNr values from SPECT/CT and PET/CT imaging.

The patients were followed-up after treatment within 3 months (2.8 mo ± 0.84) on contrast- enhanced CT to assess treatment response. The criteria for treatment response evaluation was modified RECIST (6). The responder was defined as a patient with complete or partial response and non-responder as stable and or progressive disease.

Statistical analysis:

The statistical software Statistical Package for the Social Sciences (SPSS) 20.0 and GraphPad Prism (version 8.0, GraphPad software) have been used to analyze the data. For evaluating the correlation and agreement of the TNr values, Pearson's correlation coefficient and Bland Altman plot with two-way random, average score intraclass correlation coefficient (ICC) were used. Categorical values were compared utilizing Chi-squared test or Fisher's exact test. Continuous variables following normal distribution were compared with paired t-test or repeated measure ANOVA and variables not following normal distribution with Wilcoxon signed-rank test or Friedman test. The cutoff value for absorbed dose, sensitivity and specificity for prediction of treatment response were calculated based on ROC curve from both PET/CT and SPECT/CT. The univariate logistic regression analysis was implemented to find parameters that are associated with treatment response. Significance threshold was set at $P \leq 0.05$.

RESULTS

The mean radioactivity of ^{90}Y resin microsphere injected to 34 patients (45 targeted lesions) was 2.02 (±0.75) GBq. One third (32.4%) of patients were treated with two target supplying arteries. The location of tumors on the right liver was more common than the left liver in our study (32/34 vs 2/34 patients). The number of responders was 23/34 (70.6%) which was higher than non-responders (Table 1).

Table 1. Clinical characteristic of patients (n=34)

Clinical variable	Value
Age (years, mean ± SD)	53.76±14,24
Gender	
Male	32 (94%)
Female	2 (6%)
Underlying liver disease	
Hepatitis B	33 (97%)
Hepatitis C	-
Tumor location	
Right liver	32 (94%)
Left liver	2 (6%)
Tumor size (ml, mean ± SD)	752.85 ± 630.85
Portal vein branch thrombosis	18/34 (52.9%)
Tumor necrosis	12/34(35.3%)
Barcelona stage	
Intermediate	6/34(17.6%)
Advanced	28/34(82.4%)
Number of targeted lesions	45
Tumor treated with one target supplied artery	23/34 (67.6%)
Tumor treated with two target supplied arteries	11/34 (32.4%)
Treatment response	
Response (completed and partial response)	24/34 (70.6%)
Non response (stable and progression disease)	10/34 (29.4%)
Radioactivity of ^{90}Y resin microspheres for treatment	2.02±0.75

Comparing imaging characteristics between ^{99m}Tc-MAA SPECT/CT and ^{90}Y-PET/CT

The imaging characteristics on SPECT/CT was concordant with post-treatment PET/CT although tumor thrombosis uptake was more readily found on PET/CT (figure 1 and table 2). There was no statistically significant difference between the value of LSF on SPECT/CT, PET/CT (p=0.138, repeated measures ANOVA test) and the results was same for mean of TNr (p=0.1339, Friedman test). However, the correlation (r) between TNr on SPECT/CT and PET/CT was 0.6192, (p=<0.0001, 95% of CI: 0.39-0.77). The agreement between TNr on ^{99m}Tc-MAA SPECT/CT and ^{90}Y-PET/CT (fig 2) is good.

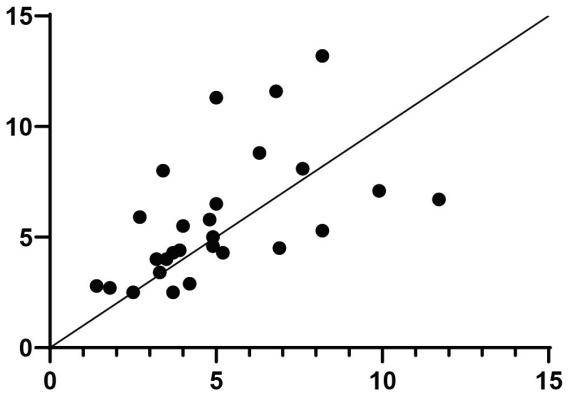

Fig1. Correlation between TNr on ^{99m}Tc-MAA planar image and ^{90}Y PET/CT

r=0.414, p=0.0148, 95% of CI: 0.08-0.66

Table 2. Imaging characteristics and parameters on ^{99m}Tc-MAA planar image, ^{99m}Tc-MAA SPECT/CT and ^{90}Y PET/CT

Tumor uptake patterns and simulation parameters	^{99m}Tc-MAA SPECT/CT	^{90}Y-PET/CT post treatment	p
Heterogeneity of tumor uptake	20/34 (58.8%)	20/34 (58.8%)	0.000
Necrotic tumor	12/34 (35.3%)	12/34 (35.3%)	0.00
Thrombosis uptake	4/34 (11.7%)	10/34 (29.4%)	0.004
Extrahepatic uptake	-	-	-
LSF (%, mean±SD)	4.31±2.42	6.02±2.06	0.99
TNr (mean±SD)	6.03±2.49	6.11±2.72	0.99

LSF: liver lung shunt fraction (%), TNr: tumor/normal liver count ratio

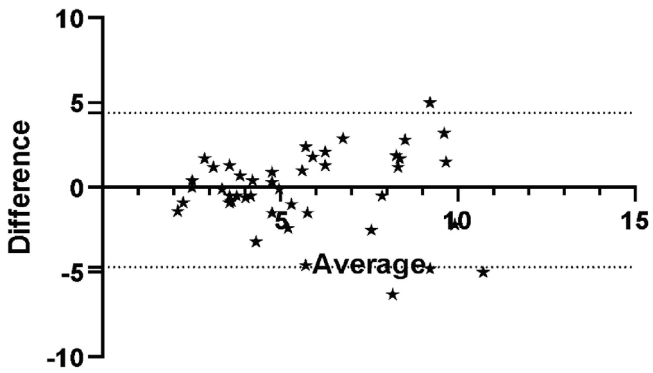

Fig2. Bland – Altman plot of agreement between TNr on ^{99m}Tc-MAA SPECT/CT and ^{90}Y-PET/CT

Bias: -0.1368, SD: 2.322, 95% of limits of agreement: -4.6 to 4.4

Value of ^{99m}Tc-MAA SPECT/CT in the prediction of treatment response

Dosimetry for targeted tumor estimated on ^{99m}Tc-MAA SPECT/CT could predict the response after treatment. Estimated absorbed dose for ^{99m}Tc-MAA SPECT/CT (fig. 4A) was significantly higher than in PET/CT (169.9 ± 49.04 vs 100.4 ± 42.69, p<0.0001, paired t-test). Meanwhile, the estimated Dtumor of responders with SPECT/CT was significantly higher than the estimated Dtumor of non-responders (178.9 ± 46.77 vs 117.78 ± 17.37, p=0.0014, paired t-test). (fig, 4B) The area under ROC curve of Dtumor estimated on ^{99m}Tc-MAA SPECT/CT is 0.850 (p<0.001, 95% of CI: 0.823 to 1) which was higher than 0.614 of Dtumor on PET/CT (p=0.008, 95% of CI: 0.636 to 0.951). However, there was no significant difference between area under ROC curve of Dtumor on SPECT/CT and planar (p=0.051, DeLong test). By analyzing the ROC curve of Dtumor (Gy), we found that Dtumor threshold of 125 Gy estimated on ^{99m}Tc-MAA SPECT/CT was the most accurate for prediction of treatment response after ^{90}Y-radioembolization in HCC patients with sensitivity of 87.5% and specificity of 90% (fig.3). The results indicated that SPECT/CT is superior to PET/CT in prediction of treatment response. Among clinical factors and parameters on ^{99m}Tc-MAA SPECT/CT, logistic regression analysis (table 4) showed only Dtumor on SPECT/CT remains significantly associated with the response (p=0.0493).

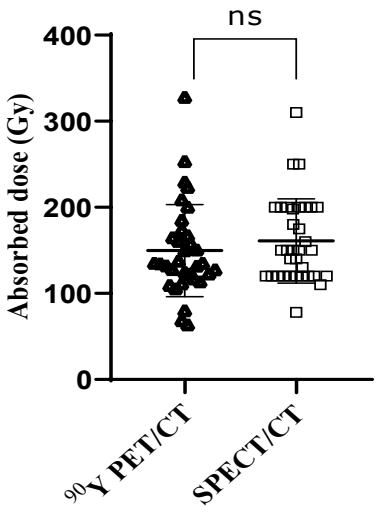

Fig3A. Comparing mean of estimated absorbed dose (Gy) to targeted tumor between ^{90}Y PET/CT and SPECT/CT

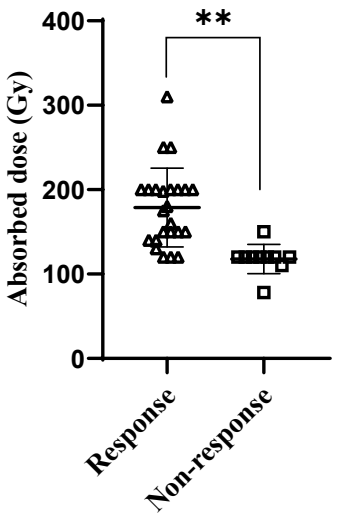

Fig3B. Comparing mean between estimated absorbed dose (Gy) to targeted tumor between responders and non-responders in SPECT/CT.

Table 4. Logistic regression analysis of factors associated with treatment response

Factors	Relative risk (CI 95%)	p
Dtumor SPECT/CT	2.059 (-0.007 to -1.297)	0.0493*
TNr on SPECT/CT	0.7562 (-0.07959 to 0.03672)	0.4561
Volume of tumor	1.217 (-0.0002118 to 0.0008288)	0.2342
Pattern of tumor uptake (homogeneous or heterogeneous)	0.4827 (-0.2557 to 0.4130)	0.6332
Portal thrombosis (yes or no)	0.9499 (-0.4340 to 0.1593)	0.3506
Barcelona stage (advanced or not advanced)	0.6340 (-0.5302 to 0.2799)	0.5314

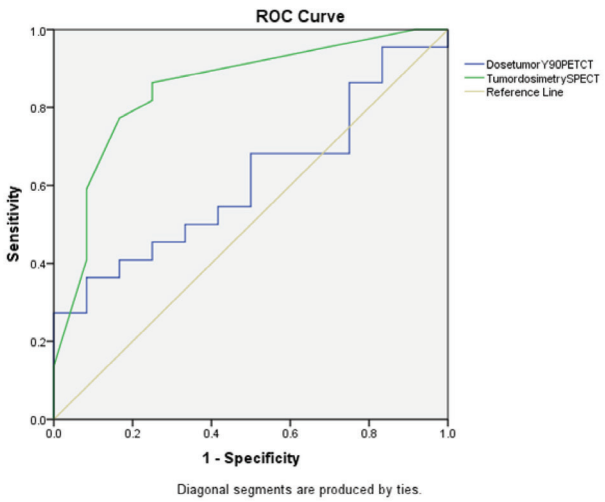

Fig 4. ROC curve for sensitivity and specificity of tumor absorbed dose on ^{90}Y-PET/CT and (blue) ^{99m}Tc-MAA SPECT/CT (green) in the diagnosis of tumor response

DISCUSSION

The first key finding of this study is that ^{99m}Tc-MAA SPECT/CT image showed stronger agreement with post-treatment ^{90}Y-PET/CT. Furthermore, dosimetry estimated on ^{99m}Tc-MAA SPECT/CT could predict treatment response with higher sensitivity and specificity than ^{90}Y-PET/CT imaging.

^{99m}Tc-MAA distribution was considered as a surrogate marker for absorbed dose of ^{90}Y - resin microspheres. In general, planar or SPECT scanning had been used widely before RE. ^{99m}Tc-MAA imaging aims for mapping the tumor feeding vessels as well as detecting the extrahepatic uptake to prevent complications due to ^{90}Y resin microspheres reflux. Another study confirmed the superior value of ^{99m}Tc-MAA SPECT/CT in detection of digestive extra hepatic uptake (7). In our study, ^{99m}Tc-MAA SPECT/CT was used as a guide for selective artery partition model dosimetry in 10/34 cases. Dosimetry by specific SPECT/CT partition model was successful to achieve the high absorbed dose to tumor and low dose to normal liver in ^{90}Y radioembolization. Besides, delineation of the volume of interest with tumor uptake, exclusion of necrotic portion of tumor and detection of extrahepatic uptake provide the basis of the tumor dosimetry. SPECT alone cannot achieve accurate volume measurement of the volume of interest (VOI) and the parameters of the simulation scan might be underestimated (8). ^{99m}Tc-MAA SPECT/CT scan is more functional and it takes into account the mass of viable tumor and non-tumorous liver better than SPECT and or planar imaging. Our study reported a higher number of cases in SPECT/CT with heterogeneous tumor uptake and necrotic tumor than planar imaging. When compared with post-radioembolization ^{90}Y-PET/CT, ^{99m}Tc-MAA SPECT/CT imaging showed the concordant results except for the detection of thrombosis uptake. ^{99m}Tc-MAA SPECT/CT showed 4/34 cases with thrombosis uptake while ^{90}Y-PET/CT detected 14/34 cases and ^{99m}Tc-MAA could not detect thrombosis uptake.

The dosimetry results of SPECT/CT have played a significant role in quantitative simulation imaging in therapeutic planning. The ratio of tumor-to-normal liver (TNr) exhibits the safety dose range for ^{90}Y-resin microsphere infusion in partition model dosimetry. The thresholds for the TNr and LSF% are the framework for efficacious planning dosimetry. Based on TNr and LSF%, ^{90}Y-resin microsphere activity could be achieved with the maximum delivery dose for target tumors while sparing normal organs. Especially for multiple lesions, the discrete ROI of targeted tumors could be defined more accurately by SPECT/CT. On ^{99m}Tc-MAA planar, TNr less than 2 could be considered as an unsafe threshold for ^{90}Y microsphere administration and SPECT/CT might be more precise in calculation. The TNr estimated on SPECT/CT was more reliable than TNr estimated on planar imaging in our study. The agreement and correlation of TNr on SPECT/CT were strong with TNr on ^{90}Y PET/CT as a reference. Furthermore by utilizing TNr, the tumoricidal dose could be estimated by the partition model individually for each tumor by calculating TNr mean for each patients and TNr for each tumor. This study proved that planar image underestimates the absorbed dose to tumor than SPECT/CT and dosimetry with SPECT/CT is more accurate for treatment response evaluation. Our study indicated that the best cutoff value of Dtumor is 125 Gy This study proved that the absorbed dose by SPECT/CT are higher than non-responders. Garin et al. reported a higher absorbed dose of responders than non-responders after ^{90}Y-TheraSphere treatment where the

minimum absorbed dose should be 205 Gy (9, 10). On the other hand, the cutoff of the tumoricidal dose among published studies to achieve radiological treatment response was discordant and it was highlighted that the absorbed dose of 120Gy is recommended for resin microsphere and was different from that of glass microsphere (11). The treatment response after ^{90}Y-TheraSphere depends not only on the tumoricidal absorbed dose but also on heterogeneity uptake, thrombosis, tumor size and stage of disease (10). In our study, the radiological treatment response depends only on delivery dose to tumor estimated by ^{99m}Tc-MAA SPECT/CT (univariate analysis, p=0.043). It could be explained that the number of patients in our study was lower than published studies assessing the treatment effect of ^{90}Y-TheraSsphere.

In our study, we could not assess the role of simulation parameters on ^{99m}Tc-MAA SPECT/CT in the prediction of overall and progression free survival for the unresectable HCC. It was challenging to follow-up longer than three months for foreign patients who visited our hospital for the treatment. Also, we could not show the association of TNr, LSF and Dtumor with tumor uptake pattern, tumor size and presence of portal vein thrombosis. There was too small number of patients in each group for statistical analysis. In addition, the method to estimate the absorbed tumor dose on ^{90}Y PET/CT need to be improved. It was recommended to use Kernel or Montecarlo stimulation tool to estimate the uniformity of absorbed doses on each part of tumor. In our study, partition method should be used for stimulation alone and probably not accurate for measuring the tumor dose.

Conclusions: This study highlights that ^{99m}Tc-MAA SPECT/CT could be a reliable simulation tool in validation with ^{90}Y PET/CT. Delivery dose to targeted tumors estimated on SPECT/CT could be the main factor to predict the radiological treatment response. Another study should be further investigated to validate the role of ^{90}Y PET/CT imaging.

Acknowledgment: We would like to thank our staffs in Nuclear Medicine, Diagnostic imaging and Gastroenterology.

Conflict of interest: none

REFERENCE

1. Zhu RX, Seto W-K, Lai C-L, Yuen M-F. Epidemiology of Hepatocellular Carcinoma in the Asia-Pacific Region. Gut and liver. 2016;10(3):332-9.
2. Ahmadzadehfar H, Sabet A, Biermann K, Muckle M, Brockmann H, Kuhl C, et al. The significance of 99mTc-MAA SPECT/CT liver perfusion imaging in treatment planning for 90Y-microsphere selective internal radiation treatment. J Nucl Med. 2010;51(8):1206-12.
3. Giammarile F, Bodei L, Chiesa C, Flux G, Forrer F, Kraeber-Bodere F, et al. EANM procedure guideline for the treatment of liver cancer and liver metastases with intra-arterial radioactive compounds. Eur J Nucl Med Mol Imaging. 2011;38(7):1393-406.
4. Gil-Alzugaray B, Chopitea A, Iñarrairaegui M, Bilbao JI, Rodriguez-Fraile M, Rodriguez J, et al. Prognostic factors and prevention of radioembolization-induced liver disease. Hepatology (Baltimore, Md). 2013;57(3):1078-87.
5. Gates VL, Esmail AA, Marshall K, Spies S, Salem R. Internal pair production of 90Y permits hepatic localization of microspheres using routine PET: proof of concept. J Nucl Med. 2011;52(1):72-6.
6. Kim MN, Kim BK, Han KH, Kim SU. Evolution from WHO to EASL and mRECIST for hepatocellular carcinoma: considerations for tumor response assessment. Expert Rev Gastroenterol Hepatol. 2015;9(3):335-48.
7. Lenoir L, Edeline J, Rolland Y, Pracht M, Raoul J-L, Ardisson V, et al. Usefulness and pitfalls of MAA SPECT/CT in identifying digestive extrahepatic uptake when planning liver radioembolization. European Journal of Nuclear Medicine and Molecular Imaging. 2012;39(5):872-80.

8. Garin E, Lenoir L, Rolland Y, Laffont S, Pracht M, Mesbah H, et al. Effectiveness of quantitative MAA SPECT/CT for the definition of vascularized hepatic volume and dosimetric approach: phantom validation and clinical preliminary results in patients with complex hepatic vascularization treated with yttrium-90-labeled microspheres. Nucl Med Commun. 2011;32(12):1245-55.

9. Garin E, Rolland Y, Laffont S, Edeline J. Clinical impact of (99m)Tc-MAA SPECT/CT-based dosimetry in the radioembolization of liver malignancies with (90)Y-loaded microspheres. European Journal of Nuclear Medicine and Molecular Imaging. 2016;43:559-75.

10. Garin E, Rolland Y, Pracht M, Le Sourd S, Laffont S, Mesbah H, et al. High impact of macroaggregated albumin-based tumour dose on response and overall survival in hepatocellular carcinoma patients treated with 90Y-loaded glass microsphere radioembolization. 2017;37(1):101-10.

11. Kao YH, Hock Tan AE, Burgmans MC, Irani FG, Khoo LS, Gong Lo RH, et al. Image-guided personalized predictive dosimetry by artery-specific SPECT/CT partition modeling for safe and effective 90Y radioembolization. J Nucl Med. 2012;53(4):559-66.

Correspondent: Mai Hong Son.
Recieved: 05/10/2021. Assessed: 20/10/2021. Reviewed: 26/10/2021. Accepted: 01/11/2021